



Absolute configuration and crystal packing chirality for three conglomerate-forming *ortho*-halogen substituted phenyl glycerol ethers

Alexander A. Bredikhin^{*}, Aidar T. Gubaidullin, Zemfira A. Bredikhina

A.E. Arbuzov Institute of Organic and Physical Chemistry, Kazan Scientific Center, Russian Academy of Sciences, Arbuzov St., 8, Kazan 420088, Russian Federation

ARTICLE INFO

Article history:

Received 4 March 2010

Received in revised form 28 April 2010

Accepted 29 April 2010

Available online 6 May 2010

Keywords:

Spontaneous resolution

Conglomerates

Molecular structure

Crystal packing

Supramolecular pattern chirality

Chirality transfer

ABSTRACT

Three conglomerate-forming *ortho*-Hal (Hal = Cl, Br, I) substituted phenyl glycerol ethers **1–3** were investigated by single-crystal X-ray analysis, and the absolute configuration for all substances was established. The molecular structures and crystal packing details for halogen derivatives were compared with the same characteristics for *ortho*-OCH₃ and *ortho*-CH₃ analogues. Two different types of crystal packing were evaluated for these very much alike compounds. The interplay of the supramolecular crystal organization chirality sense and the single molecule absolute configuration was demonstrated. Some stabilizing and destabilizing interactions involving the *ortho*-substituents were revealed. The resolution of *rac*-**2** by entrainment procedure was successfully realized.

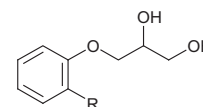
© 2010 Elsevier B.V. All rights reserved.

1. Introduction

The chirality phenomenon, origin and transformation of chiral matter, and homochiral imperative of molecular evolution are evergreen and multifold features in natural science [1]. Among all others related problems spontaneous resolution of chiral substances [2] is of special interest in so far as it has close relation to the origin of life [3] and to modern problem of economically effective nonracemic compounds production [4]. Spontaneous resolution is intimately associated with the racemic conglomerate formation. Supplementary interest to the conglomerate-forming substances has its origin in a recently discovered by Dutch investigators method in which grinding-induced attrition is used to transform racemic conglomerates virtually quantitatively into a single enantiomer [5].

In spite of the topic popularity, for nowadays the nature of spontaneous resolution, the reasons why a chiral organic substance falls on this or that side of the borderline dividing racemic compound from racemic conglomerates remain very obscure [2]. One way to gain a better understanding of the phenomenon consist of systematic investigation of the crystal structure of conglomerate-forming substances and their comparison with similar systems. In this connection in the present paper we want to establish the crystal structure as well as the absolute configuration for three

ortho-halogen substituted phenyl glycerol ethers, 3-(2-*R*-phenoxy)-propane-1,2-diols **1** (R = Cl), **2** (R = Br), and **3** (R = I).



R = Cl (**1**); Br (**2**); I (**3**); OCH₃ (**4**); CH₃ (**5**).

For all this compounds the ability to spontaneous resolution was established earlier by spectroscopy [6] and thermal analysis [7]. We want to demonstrate how the chirality sense of the primary elements (absolute configuration of the molecules) has an influence on the supramolecular solid state pattern chirality as a whole. We shall correlate crystal organization characteristics for compounds **1–3** with the like ones for chemically similar chiral drugs guaifenesin **4** and mephensin **5**. Both latter compounds prone to spontaneous resolution as it was established earlier [8]. The last purpose of our paper arises from the fact that nonracemic *ortho*-halogen substituted phenyl glycerol ethers could be used as the precursors for single enantiomer highly biologically potent benzodioxanes [9]. In the original paper the single enantiomers of phenyl glycerol ethers were synthesized from the enantiopure precursors. However, for the conglomerate-forming substances the possibility exists to apply a very effective direct racemate resolution approach [4]. It will be tested with *rac*-**2**.

^{*} Corresponding author. Tel.: +7 843 273 45 73; fax: +7 843 273 18 72.

E-mail address: baa@iopc.ru (A.A. Bredikhin).

2. Experimental

2.1. General

Optical rotations were measured on a Perkin–Elmer model 341 polarimeter (everywhere over the paper the value of specific rotation is given in $\text{deg ml g}^{-1} \text{dm}^{-1}$, and the concentration of solutions, c , appears in g/100 ml). Melting points for general purposes were determined using a Boëtius apparatus and are uncorrected.

2.2. Materials

The syntheses of the compounds **1–3** in racemic and enantiopure form are described in our preceding paper [7]. For all compounds single-crystal X-ray diffraction experiments have been performed at first with enantiopure samples in attempt to establish the absolute configuration for these compounds. The sample of (*S*)-**1**, 99.8% ee, was crystallized from CH_2Cl_2 and was characterized by mp 90–91 °C, $[\alpha]_D^{20} = -14.0$ (c 1.0, hexane/EtOH 4:1). The sample of (*R*)-**2**, 99.5% ee, was crystallized from CH_2Cl_2 and was characterized by mp 101–102 °C, $[\alpha]_D^{20} = +13.8$ (c 1.0, hexane/EtOH 4:1). The sample of (*S*)-**3**, 99.9% ee, was crystallized from CH_2Cl_2 and was characterized by mp 110–112 °C, $[\alpha]_D^{20} = -16.3$ (c 1.0, hexane/EtOH 4:1). Crystal information listed in Table 1 belongs to these samples. Other set of X-ray diffraction experiments have been performed with individual crystals picked up from the bulk racemate samples of the compounds **1–3**, mp 70–72 °C, 80–82 °C, and 90–92 °C, respectively. For all three substances the space groups and the unit cell parameters for accidentally hand-picked single crystals were identical (within the limits of experimental error) with those for enantiopure samples.

2.3. X-ray crystal structure analysis

The X-ray diffraction data for the crystals of **1–3** (see Section 2.2) were collected on a Enraf–Nonius CAD-4 automatic

four-circle diffractometer at 294 K (graphite monochromator, Cu K α (1.54184 Å) for (**1**, **2**) and Mo K α radiation (0.71069 Å) for (**3**), $\omega/2\theta$ scan method. The crystal data, data collection, and the refinement details are given in Table 1. The stability of the crystals and experimental conditions was checked every 2 h using three control reflections, while the orientation was monitored every 200 reflections by centering two standards. No significant decay was observed. Corrections for Lorentz and polarization effects and absorption correction were applied. The structure was solved by direct method using SIR [10] program and refined by the full matrix least-squares using SHELXL [11] programs. All non-hydrogen atoms were refined anisotropically. The hydrogen atoms were inserted at calculated positions and refined as riding atoms except the hydrogen atoms on hydroxyl groups which were located from difference maps and refined using a riding model. The absolute structure of the single crystals was determined on the basis of the Flack [12] parameter. All calculations were performed on PC using WinGX [13] suit of programs. Data collection and data reduction were performed on Alpha Station 200 computer using MoLEN [14] program. Analysis of the intermolecular interactions was performed using the program PLATON [15].

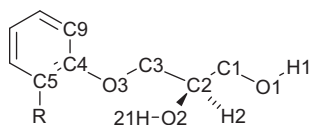
3. Discussion

3.1. Crystal structure

It comes as no surprise that three compounds having very close chemical structure have very close crystal structures too. As the data of Table 1 suggest, all the nonracemic compounds **1–3** crystallize in the same $P2_12_12_1$ space group, $Z' = 1$, having close parameters of crystal unit cell. A small and systematic b and c axes elongations in going from **1** to **3** are completely consistent with the Van der Waals radii increase for the halogen atoms. For all three compounds studied racemic samples crystallize in the same noncentrosymmetric space group $P2_12_12_1$ having almost identical parameters of crystal unit cell as for the enantiopure ones. This fact

Table 1
Crystallographic data for (*S*)-*ortho*-Cl (**1**), (*R*)-*ortho*-Br (**2**), and (*S*)-*ortho*-I (**3**) substituted phenyl glycerol ethers.

Compound formula	(1) $\text{C}_9\text{H}_{11}\text{ClO}_3$	(2) $\text{C}_9\text{H}_{11}\text{BrO}_3$	(3) $\text{C}_9\text{H}_{11}\text{IO}_3$
M (g/mol)	202.63	247.09	294.08
Temperature, K	294(2)		
Crystal class	Orthorhombic	Orthorhombic	Orthorhombic
Space group	$P2_12_12_1$	$P2_12_12_1$	$P2_12_12_1$
Crystal size	$0.24 \times 0.20 \times 0.15 \text{ mm}^3$	$0.42 \times 0.35 \times 0.18 \text{ mm}^3$	$0.32 \times 0.24 \times 0.16 \text{ mm}^3$
Z	4	4	4
Radiation type	Cu K α , 1.54184	Mo K α , 0.71069	
Cell parameters	$a = 4.900(4)$, $b = 7.5860(10)$, $c = 25.89(2) \text{ Å}$	$a = 4.873(3)$, $b = 7.669(6)$, $c = 26.510(18) \text{ Å}$	$a = 4.853(6)$, $b = 7.838(6)$, $c = 27.210(17) \text{ Å}$
$V, \text{ Å}^3$	962.4(11)	991(1)	1035(1)
$F(000)$	424	496	568
$\rho_{\text{calc}}, \text{ g/cm}^3$	1.399	1.657	1.887
$\mu, \text{ cm}^{-1}$	33.12	54.62	30.68
Extinction coefficient	0.023(8)	0.029(1)	0.006(2)
θ , deg	$9.68 \leq \theta \leq 74.34$	$6.68 \leq \theta \leq 74.07$	$2.70 \leq \theta \leq 24.65$
Reflections measured	897	1101	2570
Independent reflections	896		
$[R(\text{int}) = 0.1767]$	1101		
$[R(\text{int}) = 0.0000]$	1342		
$[R(\text{int}) = 0.1464]$			
Number of parameters/restraints	119/0	119/1	107/0
Reflections $[I > 2\sigma(I)]$	794	663	832
Flack parameter	0.00(4)	0.06(4)	0.03(9)
$R_1/wR_2 [I > 2\sigma(I)]$	0.0482/0.1255	0.0252/0.0499	0.0521/0.1126
R_1/wR_2 (all reflections)	0.0590/0.1324	0.0449/0.0551	0.1012/0.1468
Goodness-of-fit on F^2	1.068	0.947	0.732
$\rho_{\text{max}}/\rho_{\text{min}} (\text{e Å}^{-3})$	0.243/−0.221	0.110/−0.096	0.622/−0.956



Scheme 1. Partial numbering accepted for molecules **1–5**.

is consistent with our earlier conclusion concerning the conglomerate nature of racemic **1–3** [6,7].

As it follows from Table 1, the Flack parameter for the samples with negative sign of optical rotation in hexane/EtOH 4:1 is well consistent with *S*-configuration of the C2 carbon atom (the situation of chloride **1** and iodide **3**). On the same basis the positive sign of optical rotation in the identical mixed solvent corresponds to *R*-enantiomer (the case of bromide **2**).

All the molecules in the **1–3** crystals have no unusual geometric parameters and adopt very similar conformations. This conformation could be described by enumeration of torsion angles formed by non-hydrogen atoms of the common structure fragment C5C4O3C3C2C1O1 (see Scheme 1 for the accepted numbering). The torsions for compounds **1–3** found in this work are listed in Table 2 alongside with the same values earlier obtained for guaifenesin **4** and mephensin **5** [8]. For the purpose of comparison all the torsions are listed for *R*-enantiomers (the real torsions for *S*-enantiomers have opposite signs). As it follows from the Table 2 the

molecules **1–3** have almost planar shapes of all except terminal (H₂)C1O1H1 fragments.

Supramolecular pattern of crystal organization for compounds **1–3** has much in common. Let us use chlorosubstituted compound (*S*)-**1** to illustrate the type of intermolecular hydrogen bonds system in the crystal. The well pronounced motif for the (*S*)-**1** crystal lattice involves the 1D columns formed by H-bonded molecules along the 2₁ axes (*Ob*) (Fig. 1, grey zones).

For every specific column on the Fig. 1 each upper right and lower left molecules present for the intermolecular hydrogen bond columnar system their terminal primary hydroxyls, whereas lower right and upper left molecules present for the same purpose their secondary hydroxyls. The hydroxyl groups taking no part in this namely H-bond column take part in the neighbouring ones, where former “right” molecules became “left” ones and *vice versa*. As a result of simultaneous participation of every molecule in the two different 1D column formation the 2D “palisade-like” supramolecular bilayer pattern of H-bonded molecules arranged parallel to crystallographic plane *Oab* arises. All the registered details are typical of hydrogen bonds organization in guaifenesin crystals as well.

The important feature of the ascertained hydrogen bond system lies in its chirality: the succession “closest donor – closest acceptor” (...O1–H1...O2'–H21'...O1''–H1''...) organized along *Ob* axis in the crystals of (*S*)-**1** and (*S*)-**3** gives rise to right-handed *P*-helix. This phenomenon could be seen in the Fig. 1 for (*S*)-**1**; for the best examination the same 1D column enlarged image is given in the

Table 2

The principal torsion angles (see Scheme 1 for the numbering) for (*R*)-enantiomers of the compounds **1–3** (this work) and **4–5** (Ref. [8]).

Torsions	Compounds					
	1	2	3	4	5, Molecule B	5, Molecule A
C5C4O3C3	178.9(3)	179.9(3)	177.2(12)	174.9(1)	–177.9(2)	–179.8(2)
C4O3C3C2	175.5(3)	174.9(3)	175.1(10)	177.7(1)	–175.1(1)	–175.1(2)
O3C3C2C1	53.3(3)	51.8(4)	55.4(13)	54.1(1)	65.3(2)	–59.6(2)
C3C2C1O1	52.0(3)	52.9(4)	55.0(13)	51.2(1)	60.6(2)	–60.5(2)
O3C3C2O2	176.9(2)	177.0(3)	178.8(9)	177.23(9)	–172.6(1)	64.1(2)
RC5C4O3	0.3(4)	1.6(5)	3.4(17)	–	3.7(3)	0.5(3)

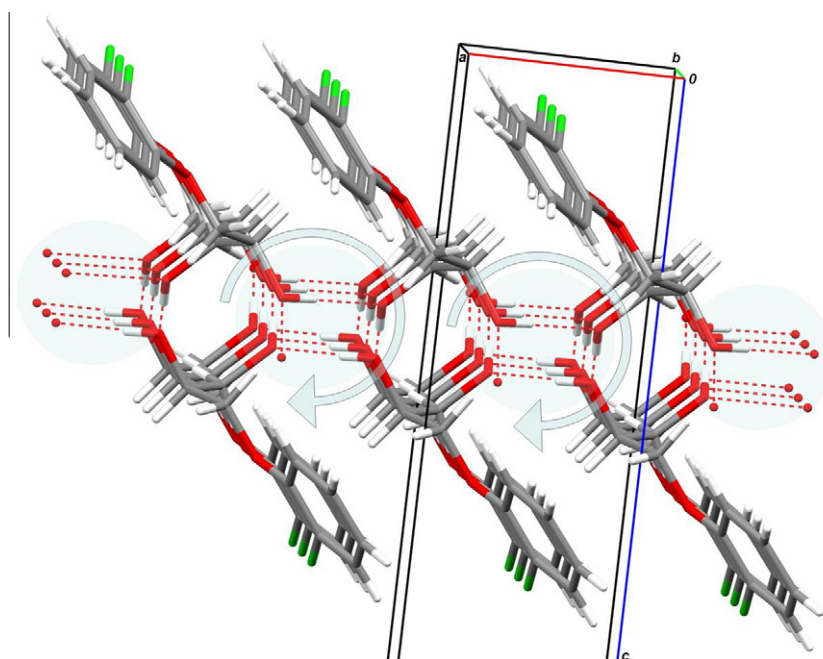


Fig. 1. 1D H-bonded columns (grey zones) jointed into 2D “palisade-like” supramolecular bilayer pattern in the (*S*)-**1** crystals, intermolecular hydrogen bonds denoted by dashed lines.

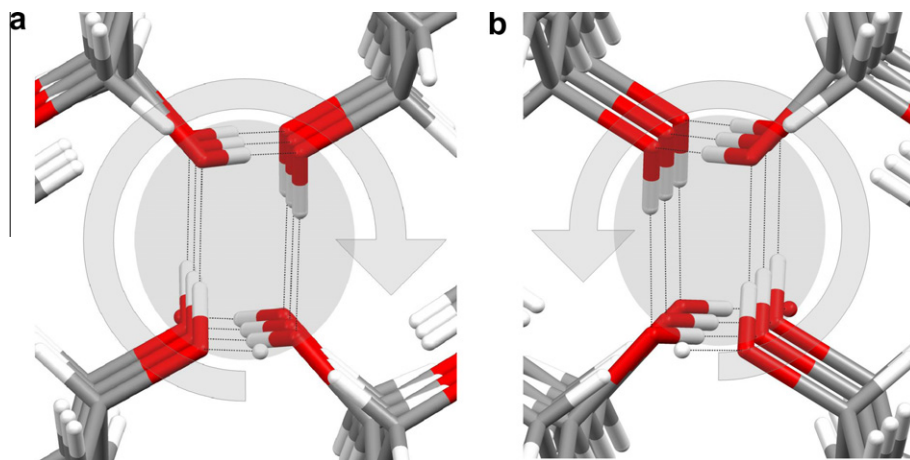


Fig. 2. 1D H-bonded columns (grey zone): (a) *P*-helix in the compound (*S*)-**3** crystals, (b) *M*-helix in the compound (*R*)-**2** crystals; intermolecular hydrogen bonds are denoted by dashed lines.

Fig. 2a for (*S*)-**3**. Having an opposite as compared to (*S*)-**1** and (*S*)-**3** configuration, molecules in the (*R*)-**2** crystalline sample adopt not an equal but mirror conformation. This in turn causes that the whole hydrogen bond pattern for (*R*)-**2** is mirror image of the other two. The same succession “closest donor–closest acceptor” in this case forms left-handed *M*-helix (grey zone in the Fig. 2b). Thus, in the case of conglomerate-forming *ortho*-halogen substituted phenyl glycerol ethers we have an expressive example of chirality transfer from the lowest level of single molecule to the level of supramolecular organization of the crystal as a whole.

The supramolecular organization of the halogen derivatives **1–3** closely matched the one of guaifenesin **4**; among other things the *M*-helix character of the H-bonded columns was also recognized for (*R*)-**4** [8]. At the same time, for the very close to *o*-Hal substituted phenyl glycerol ethers *o*-Me derivative (mephenesin, **5**), retaining the conglomerate-forming nature, quite a different crystal lattice is observed. Mephenesin crystallizes in $P2_1$ space group with two symmetry independent molecules A and B having different conformations (Table 2, Fig. 3) in the unit cell [8]. The main supramolecular motifs for crystals **5** are 1D columns aligned around 2_1 screw axes parallel with Ob axis (Fig. 3, grey zones). The central part of this column is formed by developed system of intermolecular hydrogen bonds and is hydrophilic in nature. The columns are linked with one another only through hydrophobic and/or dispersion interactions of the vast periphery formed mainly by *o*-tolyl fragments (Fig. 3).

Both **A** (red¹ in the Fig. 3) and **B** independent molecules take part in the intermolecular hydrogen bonding. Within the marked fragment in the Fig. 3 upper and lower stacks are formed by **A** molecules (let us denote them using low indices **up** and **lw**), while the left and right stacks are formed by **B** molecules (denoted by **l** and **r** indices by analogy). Concerning the intermolecular hydrogen bond pattern, the succession “closest donor – closest acceptor” is more intricate in the case of mephenesin than in the cases of the above analyzed compounds **1–4**. Fig. 4 (enlarged marked zone of Fig. 3) illustrates this pattern in more details.

It is obvious from the Fig. 4 that the sequence $O1A_{up} - H1A_{up} \cdots O2B_r - H21B_r \cdots O1B'_r - H1B'_r \cdots O2A'_{lw} - H21A'_{lw} \cdots O1A_{lw} - H1A_{lw} \cdots O1B_l - H1B_l \cdots O2B'_l - H21B'_l \cdots O2A'_{up} - H21A'_{up} \cdots O1A_{up} - H1A_{up} \cdots$ constitutes full *P*-helix pitch. Note, that in the case of mephenesin eight molecules fall inside of one helix pitch instead

of four molecules in the case of guaifenesin **4** and its halogen analogues **1–3**, and the *R*-molecules packing gives rise to right-handed *P*-helix, whereas *R*-molecules of the compounds **2** and **4** form left-handed H-bond *M*-helices in their crystals.

Thus, for the conglomerate-forming aryl glycerol ethers the crystal lattice types are divisible into two groups which could be called as guaifenesin-like and mephenesin-like. The last one contains two symmetry independent molecules ($Z' = 2$) in the unit cell. The reasons and consequences of the presence of multiple molecules in the crystal asymmetric unit were hotly debated [16]. High- Z' structures have been described as “snapshot pictures” and also as “fossil relics” of early stages in crystallization. Such a structures could be treated as inferior to the closely related $Z' = 1$ ones for a number of reasons. Analyzing the factors that may lead to the appearance of structures with $Z' > 1$, Steed points on the occurrence of a small number of strongly intermolecularly interacting functionalities, especially if unevenly distributed over the molecular surface and on the frustration between the requirements of close packing and satisfaction of intermolecular interactions of strongly interacting functionalities [16b].

Because of no fragment other than *ortho*-substituent distinguishes one compound from another in the **1–5** series, we have focused our attention on the intermolecular interactions involving these substituents. Let us analyze from this point of view the crystal structure of the chlorine derivative **1**. We have used the Mercury program package [17] for short contacts search and identification. No short contacts involving chlorine atom have been revealed when the constrain of shorter or equal of the sum of Van der Waals radii (subsequently referred to as SVDWR) distance between contacting atoms has been used. Under the constrain of $SVDWR + 0.1 \text{ \AA}$ the first contact comes to light between Cl atom and H2 secondary alcohol group methyne atom of neighbouring molecule ($-1 + x, y, z$), belonging to the same “palisade-like” supramolecular bilayer pattern (see above). In Fig. 5 these contacts are denoted by blue dashed lines and are visualized by spacefill style in the bottom part. If the constrain of $SVDWR + 0.2 \text{ \AA}$ was used, another type of C–H \cdots Cl short contacts emerge, namely between *para*-C_{ar}–H atoms H7 of a certain bilayer and Cl atoms of the neighbouring one ($-1/2 + x, 3/2 - y, 1 - z$). In Fig. 5 these contacts are denoted by red dashed lines and are visualized by spacefill style in the middle. Only when constrain $SVDWR + 0.3 \text{ \AA}$ was applied the short contacts between chlorine atoms ($-1/2 + x, 2 - y, 1 - z$) and ($1/2 + x, 2 - y, 1 - z$) belonging to neighbouring bilayers appear; in Fig. 5 these contacts are denoted by green dashed lines and are visualized by spacefill style in the upper part. It is well

¹ For interpretation of color in Figs. 1–6, the reader is referred to the web version of this article.

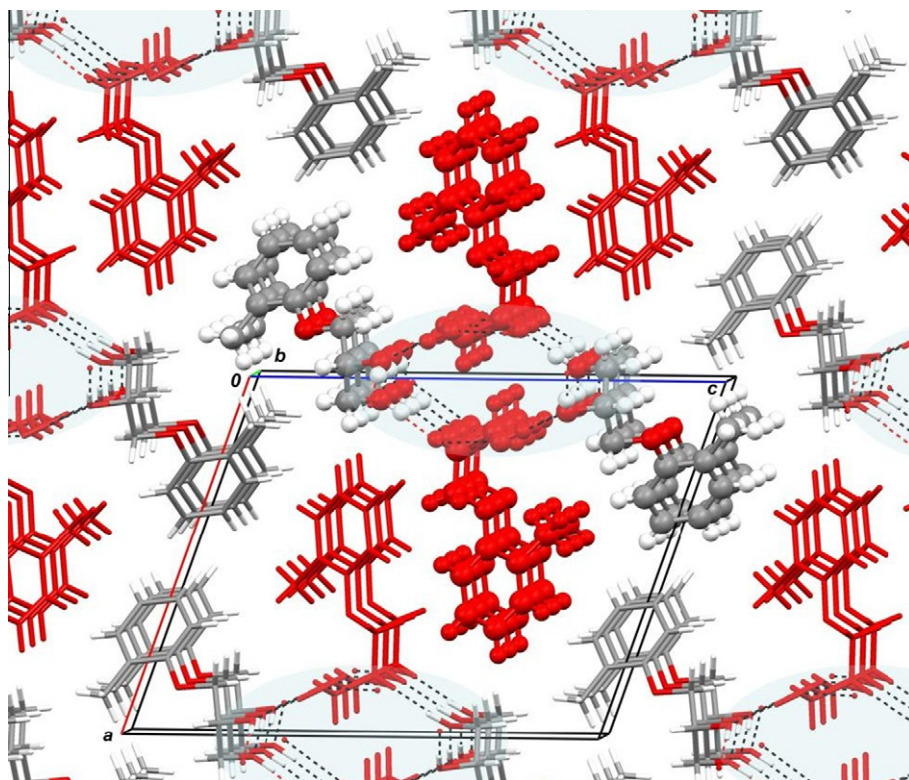


Fig. 3. 1D H-Bonded column (marked by bold style) surrounded by the same ones in the crystal of compound **5** (viewed along the $0b$ axis, A molecules denoted by red colour).

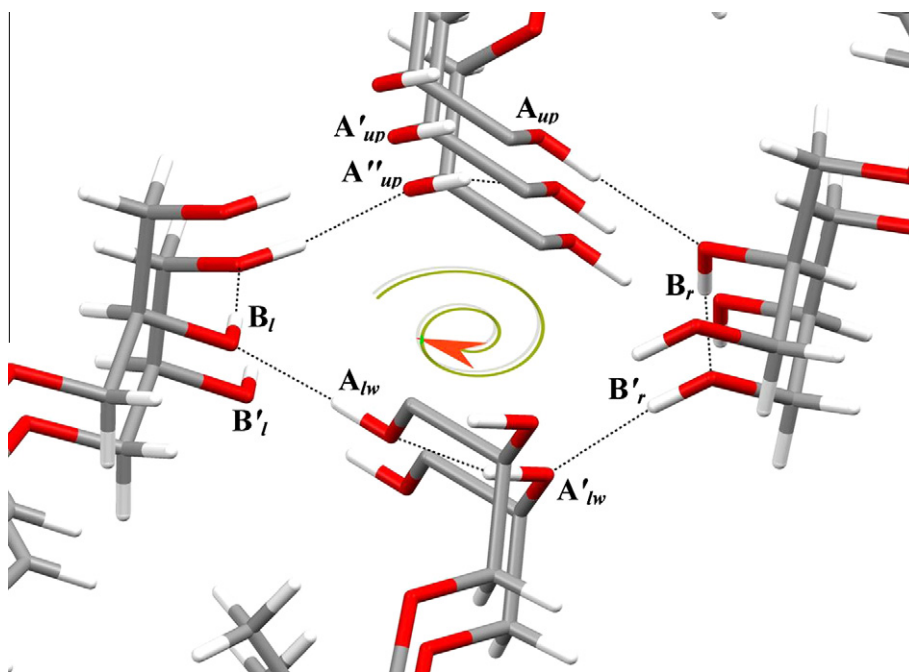


Fig. 4. The detailed view of the intermolecular hydrogen bond pattern in the (*R*)-**5** crystal. Some of the hydrogen atoms taking no part in the hydrogen bonds are omitted for clarity.

known that (moderately) short contacts of the C–H...Hal type are stabilizing in nature and could be treated as the non-classical hydrogen bonds [18]. Almost the same statement can also be made about the halogen...halogen interactions [19]. So, all the revealed chlorine noncovalent contacts stabilize the compound **1** crystal lattice.

The same is true for all other variable substituents (Br and I atoms and oxygen atom of OCH₃ group) in the guaifenesin-like crystal lattice forming compounds **2–4**. But the situation changes if the CH₃ group replaces for example chlorine atom within the same, i.e. the compound **1**, crystal lattice. To obtain this hypothetical structure the Cl atom has been replaced by carbon atom of CH₃

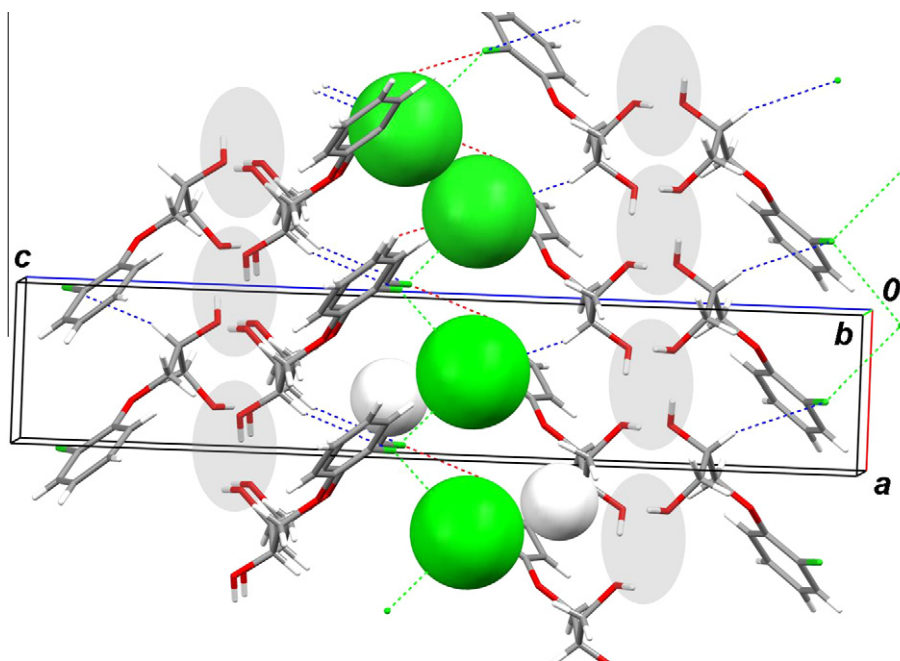


Fig. 5. The main short contacts involving chlorine atom in the compound **1** crystal. See text for details.

group in the files for *o*-Cl substituted compound on the last stages of refinement. The distance C–C(H₃) was constrained to standard value, the hydrogen atoms were inserted at calculated positions of CH₃ group and were refined using a riding model. Then the structure was refined (10 cycles) and the cif-file of the hypothetical “guaifenesin-like mephensin” was generated.

Two from the three above analyzed for Cl atom contacts are retained for CH₃ group in this hypothetical structure. These are CH₃...H₃C (−1/2 + *x*, 3/2 − *y*, −*z*) and (1/2 + *x*, 3/2 − *y*, −*z*) and HOC–H...H₃C (1 + *x*, *y*, *z*) short contacts; both types are illustrated in Fig. 6. Two substantial reasons must be taken into account during the analysis of these contacts consequences. Firstly, both H atom and CH₃ group have much in common, they bear rather positive than negative charge, they are rather electrophilic than nucleophilic. Secondly, the distances between two carbon atoms for the CH₃...H₃C contact (3.77 Å) and between H and C atoms for the HOC–H...H₃C contact (2.99 Å) are sufficiently smaller than SVDWR (4.0 Å and 3.2 Å correspondingly). Hence, the interactions in question are strongly destabilizing in nature. The packing indices for the real prototype structures **1–3** are already as low as 67.7%,

67.6%, and 66.7%. Hence, further displacements of the molecules within the bilayer or of the bilayers themselves in attempt to relax CH₃ group contacts would result in complete destruction of the crystal. In our opinion, therein lies the answer to the mephensin-like lattice arising.

3.2. Resolution of 3-(2-bromophenoxy-)propane-1,2-diol, *rac*-**2**, by entrainment procedure

Racemates resolution by entrainment [4] is a gratifying labor since success allows one to obtain easily both enantiomers without resorting to any enantiopure auxiliaries. But even in the case of conglomerate-forming substances it is not always easy to use the benefits of a spontaneous resolution. Coquerel and coworkers [4,20] are of the opinion that almost half of conglomerate-forming compounds would demonstrate poor entrainment characteristics.

Discovering new conglomerates in the family of aryl glycerol ethers we decided to examine their abilities for preferential resolution. This task was all the more interesting since *scal*-3-(2-halogenphenoxy)-propane-1,2-diols, as it was mentioned in the

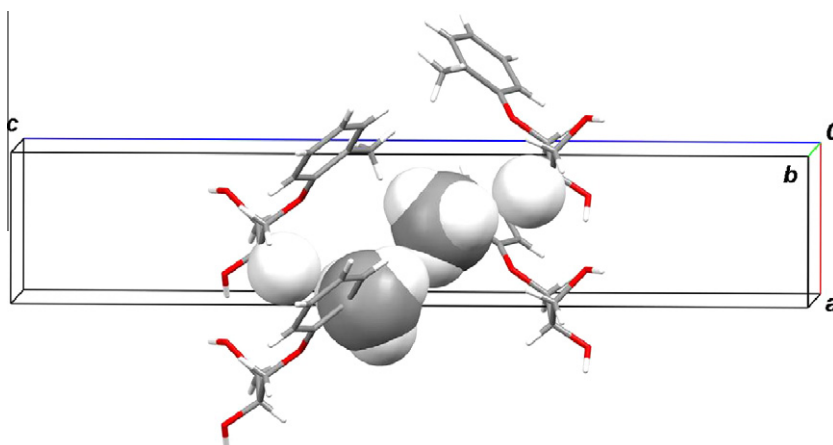
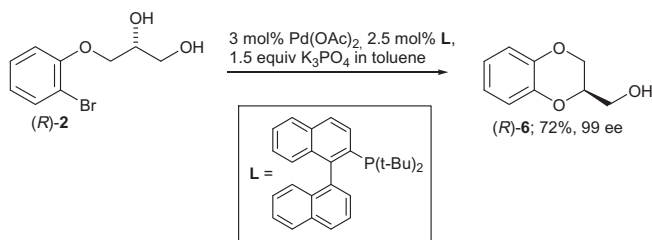


Fig. 6. The main short contacts involving CH₃ groups of mephensin molecules in the guaifenesin-like crystal lattice. See text for details.

introduction section, were already used for the very potent bioactive substances preparation. Thus *R*-**2** was smoothly converted to *R*-2-hydroxymethylbenzo-1,4-dioxane *R*-**6** with good yield and high enantiomeric excess [9]:



In the original paper the compound *R*-**2** was synthesized from the enantiopure precursor. Using the racemic sample of the compound **2** as an example we have examined entrainment effect for this class of compounds.

Over the course of the resolution a supersaturated solution of diol *rac*-**2** (3.65 g), including a moderate excess of (*R*)-**2** (0.55 g), was prepared by heating the mixture in 40 ml of EtOH/H₂O (4:6, v/v) at 40 °C. The solution was cooled to 20 °C and a small amount (15 mg) of finely pulverized seed crystals of (*R*)-**2** was added. The stirred solution was allowed to crystallize for about 75 min at 17 ± 1 °C. For monitoring the entrainment process during seed-induced crystallization of oversaturated slightly nonracemic solutions we have used optical rotation of mother liquor aliquots controlled by polarimetry. Precipitated (*R*)-**2** was collected by filtration. The weight of (*R*)-**2** obtained after filtration (0.96 g after drying; 91% ee) was more than the common weight of the initial excess of the (*R*)-enantiomer and seed added. The extra portion of *rac*-**2** (0.95 g) was then dissolved in the mother liquor at 40 °C in order that the overall quantity of **2** in the solution could be recovered. The mixture was heated until the solid was completely dissolved and then cooled to 20 °C. After the addition of (*S*)-**2** (15 mg) as seed crystals to the solution, and stirring the mixture for 80 min at 17 ± 1 °C, (*S*)-**2** (0.78 g after drying; 80% ee) was collected by filtration. Further resolution was carried out at 17 ± 1 °C by adding amended amounts of *rac*-**2** to the filtrate in a manner similar to that described above. After second cycle, 0.55 g of (*R*)-**2** (82% ee) and 0.45 g of (*S*)-**2** (78% ee) were collected.

As evident from this example, four runs (2 cycles) are sufficient to obtain from 5.9 g of racemate (*R*)- and (*S*)-**2** samples of about 1.0 g each. A high degree of enantiomeric purity of collected diols can be achieved by simple recrystallization. Making sure that the compound **2** is quite capable of preferential crystallization we made no attempts to optimize experimental conditions for the resolution.

4. Conclusions

The three *ortho*-halogen substituted phenyl glycerol ethers studied crystallize in a homochiral mode both in enantiopure (in which case the compounds have no other possibilities) and in racemic form. This fact could be treated as a last proof of spontaneous resolution for these compounds. The technique of resolution by entrainment, which leans upon this phenomenon, was successfully employed to obtain both individual enantiomers of bromine derivative **2**. During the comparison studies of the crystal structures within the *ortho*-substituted phenyl glycerol ethers family, two different crystal packing types, guaifenesin-like and mephnesin-

like, for these conglomerate-forming compounds were identified. Supramolecular 1D motifs, H-bonded columns for both types, go back to homochiral spirals, but the links between the absolute configuration of the molecules and the chirality sense of their crystal forming supramolecular ensembles are opposite. Whereas for guaifenesin-like lattice (*R*)-molecules give rise to left-handed helix, for mephnesin-like lattice (*R*)-molecules give rise to right-handed helix. Some proposals were made about the nature of intermolecular interactions stabilizing and/or destabilizing of one or other type of crystal packing.

5. Supplementary materials

Crystallographic data (excluding structure factors) for the structures reported in this paper have been deposited in the Cambridge Crystallographic Data Centre as supplementary publication Nos. CCDC 767,905 for **1**, 767,907 for **2**, and 767,906 for **3**. Copies of the data can be obtained free of charge upon application to the CCDC (12 Union Road, Cambridge CB2 1EZ UK. Fax: (internat.) +44 1223/336 033; E-mail: deposit @ccdc.cam.ac.uk).

Acknowledgement

The authors thank the Russian Fund of Basic Research for financial support (Grant number 09-03-00308).

References

- [1] [a] W.J. Lough, I.W. Wainer (Eds.), *Chirality in Natural and Applied Science*, Blackwell/CRC Press, Oxford, 2003; [b] G.H. Wagnière, *On Chirality and the Universal Asymmetry – Reflections on Image and Mirror Image*, HCA-Wiley/VCH, Zürich, 2007; [c] A. Guijarro, M. Yus, *The Origin of Chirality in the Molecules of Life. A Revision from Awareness to the Current Theories and Perspectives of this Unsolved Problem*, Royal Society of Chemistry, Cambridge, 2008.
- [2] [a] L. Perez-Garcia, D.B. Amabilino, *Chem. Soc. Rev.* 31 (2002) 342; [b] L. Perez-Garcia, D.B. Amabilino, *Chem. Soc. Rev.* 36 (2007) 941.
- [3] M. Avalos, R. Babiano, P. Cintas, J.L. Jimenez, J.C. Palacios, *Origins Life Evol. Biosphere* 34 (2004) 391.
- [4] G. Coquerel, *Top. Curr. Chem.* 269 (2007) 1.
- [5] W.L. Noorduin, E. Vlieg, R.M. Kellogg, B. Kaptein, *Angew. Chem. Int. Ed.* 48 (2009) 9600.
- [6] A.A. Bredikhin, Z.A. Bredikhina, S.N. Lazarev, D.V. Savel'ev, *Mendeleev Commun.* 13 (2003) 104.
- [7] A.A. Bredikhin, Z.A. Bredikhina, F.S. Akhatova, D.V. Zakharychev, E.V. Polyakova, *Tetrahedron: Asymmetry* 20 (2009) 2130.
- [8] A.A. Bredikhin, A.T. Gubaidullin, Z.A. Bredikhina, D.B. Krivolapov, A.V. Pashagin, I.A. Litvinov, *J. Mol. Struct.* 920 (2009) 377.
- [9] S. Kuwabe, K.E. Torrance, S. E. Buchwald, *J. Am. Chem. Soc.* 123 (2001) 12202.
- [10] A. Altomare, G. Cascarano, C. Giacovazzo, D. Viterbo, *Acta Crystallogr. A* 47 (1991) 744.
- [11] G.M. Sheldrick, *SHELXL97 a Computer Program for Crystal Structure Determination*, University of Göttingen, 1997.
- [12] [a] H.D. Flack, *Acta Crystallogr. A* 39 (1983) 876; [b] H.D. Flack, G. Bernardinelli, *J. Appl. Crystallogr.* 33 (2000) 1143.
- [13] L.J. Farrugia, *J. Appl. Crystallogr.* 32 (1999) 837.
- [14] L.H. Straver, A.J. Schierbeek, MOLEN, *Structure Determination System*, Program Description, Nonius B.V. Delft, Netherlands, vol. 1, 1994, p. 2.
- [15] A.L. Spek, *Acta Crystallogr. A* 46 (1990) 34.
- [16] [a] T. Steiner, *Acta Crystallogr. B* 56 (2000) 673; [b] J.W. Steed, *CrystEngCom* 5 (2003) 169; [c] G.R. Desiraju, *CrystEngCom* 9 (2007) 91; [d] J. Bernstein, J.D. Dunitz, A. Gavezzotti, *Cryst. Growth Des.* 8 (2008) 2011.
- [17] I.J. Bruno, J.C. Cole, P.R. Edgington, M.K. Kessler, C.F. Macrae, P. McCabe, J. Pearson, R. Taylor, *Acta Crystallogr. B* 58 (2002) 389.
- [18] [a] L. Brammer, E.A. Bruton, P. Sherwood, *Cryst. Growth Des.* 1 (2001) 277; [b] J.-A. van der Berg, K.R. Seddon, *Cryst. Growth Des.* 3 (2003) 643.
- [19] [a] B.K. Saha, A. Nangia, J.-F. Nicoud, *Cryst. Growth Des.* 6 (2006) 1278; [b] C.B. Aakeroy, M. Fasulo, N. Schultheiss, J. Desper, C. Moore, *J. Am. Chem. Soc.* 129 (2007) 13772; [c] P. Metrangolo, F. Meyer, T. Pilati, G. Resnati, G. Terraneo, *Angew. Chem. Int. Ed.* 47 (2008) 6114.
- [20] F. Dufour, G. Perez, G. Coquerel, *Bull. Chem. Soc. Jpn.* 77 (2004) 79.